Turbulent Mixing with Chemical Reaction in the Planetary Boundary Layer

R. I. SYKES, S. F. PARKER, AND D. S. HENN

ARAP Group, Titan Research and Technology Division, Titan Corporation, Princeton, New Jersey

W. S. LEWELLEN

Physics and Atmospheric Science, Drexel University, Philadelphia, Pennsylvania

(Manuscript received 30 March 1993, in final form 13 July 1993)

ABSTRACT

Detailed statistics of the fluctuating concentration field produced by large-eddy simulations (LES) of the chemically reactive mixing of two species in a convectively driven mixed layer are presented. The effect of the turbulent mixing on the effective reaction rate between the species is analyzed. The segregation between the species is shown to be significant for fast reactions, and therefore correct model predictions of the evolution of the species concentration requires an estimate of the segregation coefficient. Some simple modeling concepts for one-point second-order turbulence closure schemes are examined and compared with the LES results. The results are a promising indication that second-order closure schemes can be extended to provide a practical calculation of the turbulent mixing effects on fast chemical reactions.

1. Introduction

The study of the chemical composition of the atmosphere and its changes due to anthropogenic emissions has led to the consideration of very sophisticated chemical reaction mechanisms (Seinfeld 1986; Seigneur et al. 1985; Carter and Lurmann 1991). It is becoming increasingly recognized that although these models include many reaction pathways for species transformation their treatment of the atmospheric mixing processes is generally very crude. Chemical reaction requires intimate mixing of the species at the molecular scale, while atmospheric dispersion is effected primarily by large-scale turbulent eddies with a nonlinear cascade process resulting in the microscale mixing. This mechanism has long been shown to control combustion processes (Donaldson and Hilst 1972a; Hilst et al. 1973) and was discussed in the context of atmospheric reactions by Donaldson and Hilst (1972b). A measure of the importance of the turbulent mixing in controlling the reaction rate is the Damköhler number, the ratio of the chemical reaction rate to the turbulent mixing rate. If the reaction rate is fast in comparison with the mixing rate, then the species cannot be brought together sufficiently fast by the turbulent cascade process and the overall rate of reaction will be controlled by the turbulence timescales. These effects have been modeled empirically in the plume models of Arrelano et al. (1990) and Bange et al. (1991).

A more fundamental approach to the study of turbulent mixing with chemical reaction is afforded by large-eddy simulation (LES) where the large-scale, energy-containing eddies are resolved explicitly in a three-dimensional, time-dependent numerical simulation of the flow field. The technique has been applied to the study of surface-area sources by Schumann (1989), and local plume sources by Sykes et al. (1992). These studies were limited to the simple binary reaction, $NO + O_3 \rightarrow NO_2 + O_2$, which has a relatively fast timescale. The effect of the turbulent mixing, as measured by the segregation coefficient s where

$$s = \frac{\overline{c_u' c_d'}}{\bar{c}_u \bar{c}_d},$$

was demonstrated to be important in both studies. Here, c_u and c_d are the local concentrations of the upward- and downward-diffusing reacting species. The overbar denotes an ensemble average value, either spatial or temporal, and the prime denotes a fluctuation from the average. Thus the average reaction rate is given by

$$k\overline{c_u c_d} = k(\bar{c}_u \bar{c}_d + \overline{c_u' c_d'}) = k(1 + s)\bar{c}_u \bar{c}_d,$$

where k is the rate coefficient, assumed constant here for simplicity. For a fast reaction, the two reactants

Corresponding author address: Dr. Stephen F. Parker, ARAP Group, Titan Research and Technology, Titan Corporation, 50 Washington Road, P.O. Box 2229, Princeton, NJ 08543-2229.

will not, in general, be simultaneously nonzero, creating a strong negative correlation between the species, and s will be close to -1. The effective reaction rate will therefore be very much slower than that based solely on the mean concentrations $k\bar{c}_u\bar{c}_d$. Hilst et al. (1973) have shown that even moderate values of the correlation coefficient ρ, where

$$\rho = \frac{\overline{c'_u c'_d}}{(\overline{c'^2_u}\,\overline{c'^2_d})^{1/2}}$$

can produce large errors in the predicted reaction rate when $[(\overline{c'^2_u}/\bar{c}_u^2)(\overline{c'^2_d}/\bar{c}_d^2)]^{1/2} > 1$, particularly if ρ and therefore $s < 0$.

The correct description of atmospheric reaction mechanisms clearly requires a prediction of the segregation coefficient s. A natural framework for such a prediction is provided by second-order closure methods, which seek to develop moment equations for second-order, one-point fluctuation correlations such as $\overline{c'_u c'_d}$. The nonlinearity of the chemical reaction term produces an infinite hierarchy of moment equations, in exactly the same manner as the quadratic nonlinearity of the advective term, leading to the usual closure problem of prescribing the unknown moments in terms of the known lower-order moments at the chosen level of closure. In the present study, we shall utilize the explicit representation of the fluctuating concentration fields from large-eddy simulation of the turbulent boundary layer to provide insight into these higher-order terms. We examine several models for the triple scalar correlation and compare them with the LES results. We also implement the models in a simple one-dimensional second-order closure calculation of the convective boundary layer.

2. Review of the LES model

The LES model used in this study has been applied to a number of different flows including a neutral boundary layer (Sykes and Henn 1992), buoyancy-driven flow between horizontal plates (Sykes and Henn 1989), and a convective boundary layer (CBL) capped by an overlying stable layer (Henn and Sykes 1992), the flow of primary interest here. As the last two references give a detailed description of the model in buoyancy-driven flow, only a brief description will be given here. Henn and Sykes (1992) also show that the LES model results are in good agreement with the water tank experiments of Willis and Deardorff (1974) and other LES models.

The model is based on the spatially filtered, incompressible Navier–Stokes equations for a Boussinesq fluid. Second-order accurate finite-difference equations with leapfrog time differencing are used to solve for the velocity components (u, v, w), corresponding to the coordinate axes (x, y, z). The equation for the perturbation potential temperature θ was solved using the piecewise parabolic method (PPM) described in Carpenter et al. (1990) and Collela and Woodward (1984), employing first-order time splitting. The subgrid fluxes are computed using eddy viscosity and diffusivity models, which are functions of the subgrid kinetic energy and a filter scale. A transport equation is solved for the subgrid kinetic energy $q^2/2$ and the subgrid viscosity is modeled as

$$\nu_t = S_m q \Lambda,$$

where S_m is a stability function, similar to that derived by Mellor and Yamada (1974) but determined from the second-order closure model of Lewellen (1977). The filter scale Λ is prescribed as in Henn and Sykes (1992) as

$$\frac{1}{\Lambda^2} = \frac{1}{(0.65z)^2} + \frac{1}{\Lambda_{\max}^2}$$

providing a linear behavior near the surface and a consistent match with the turbulence closure model at the wall.

The model must also solve the conservation equations for the two reacting species:

$$\frac{\partial c_u}{\partial t} + \frac{\partial}{\partial x_i}(u_i c_u) = \frac{\partial}{\partial x_i}\left(K_t \frac{\partial c_u}{\partial x_i}\right) - k c_u c_d$$

and similarly for c_d, where K_t is the subgrid diffusivity defined as

$$K_t = S_H q \Lambda$$

and S_H is the appropriate stability function for the scalar flux. The scalar conservation equations are solved using the same PPM scheme used to solve the equation for θ. The scalar field is first advanced from time level t, to an intermediate value $\hat{c}$ using the advection and diffusion terms only. The chemical reaction term is then evaluated using a simple first-order approximation, suitably limited to ensure positive concentrations, to complete the advance to the next time level. Thus,

$$c_u^{t+1} = \hat{c}_u - S, \quad c_d^{t+1} = \hat{c}_d - S;$$

$$S = \min(k\hat{c}_u\hat{c}_d\Delta t, \hat{c}_u, \hat{c}_d),$$

where Δt is the time step. We assume that any subgrid reaction effects are negligible, which is equivalent to assuming perfect mixing within a grid volume.

Periodic lateral boundary conditions are imposed on all the dependent variables. A constant uniform heat flux H_0 is specified on the bottom surface and Monin–Obukov similarity relations are used to set temperature and velocity on the first grid point above the surface. The surface roughness is 0.1 m. A fixed surface flux E is specified for c_u, while a zero surface flux is specified for c_d. The top boundary conditions are free slip for the horizontal velocities, a constant potential temperature gradient Γ, and zero slope for the reacting scalars. The vertical velocity is damped to zero near the top boundary to prevent wave reflections.

3. LES results with a binary reaction

a. Simulation conditions

The convective boundary layer is first allowed to establish a fully developed turbulent flow field before the reacting scalar calculation is begun. Initial conditions for the CBL are specified as zero velocity and a uniform potential temperature up to an initial inversion height of $z_{i0} = 900$ m with a gradient of $\Gamma = 0.01°\text{C m}^{-1}$ above this level. A constant surface heat flux is specified as $H_0 = 0.03°\text{C m s}^{-1}$ in temperature units, equivalent to about 40 W m^{-2}. The convective velocity scale w_*, defined using H_0 and a final inversion height of 1000 m, is approximately 1 m s^{-1}. Turbulent flow is initiated by a small random perturbation to the temperature field applied below z_{i0}, and the dynamic simulation is run for 6000 s, or about $6z_i/w_*$, to establish a fully developed turbulent flow field.

Following the establishment of the convective turbulence, the scalar calculation is begun at $t = 0$. At this time, c_u is initialized as zero everywhere, while c_d is 1.0 above z_{i0} and 0.4 below. The concentration units are arbitrary, but the relative magnitudes correspond to the reference case of Schumann (1989). The surface flux of c_u is constant over the lower boundary with a value $E = 0.05$ m s^{-1}.

The nondimensional reaction rate, or Damköhler number, is defined by Schumann (1989) as

$$R = kz_i \frac{c_u^*}{w_*}$$

and represents the ratio of the reaction timescale $(kc_u^*)^{-1}$ to the turbulent convective eddy timescale $z_i w_*^{-1}$. The scalar concentration scale is defined as $c_u^* = Ew_*^{-1}$. As we shall see below, these scales are an appropriate measure for a chemical reaction rate controlled by the upward flux of c_u. The boundary layer is preloaded with c_d, making it available in abundance. We consider three cases: $R = 0.1$, 1, and 10 spanning the range from slow to fast reaction rates. Note that E is fixed in this study so that the variation in R represents a variation in k only.

The LES calculations were performed using a 48 × 48 × 61 point grid representing a 4 km × 4 km × 4 km domain. The horizontal grid spacings are uniform at 83.3 m, but the vertical grid is nonuniform, with a spacing of 10 m at the surface, 40 m in the boundary layer, and 25 m at the inversion. The time step was 4 s for most of the calculations, and the subgrid turbulence length scale $\Lambda_{\max}$ was 45 m. One high-resolution calculation was made to test convergence of the LES, particularly with regard to the neglect of subgrid species fluctuations in the chemical reaction term. This used a mesh of 80 × 80 × 72 points in the same domain as the standard resolution giving a horizontal grid of 50 m and a vertical grid of 30 m in the boundary layer. The turbulent length scale was 25 m.

b. Results

A surface release into the convective boundary layer is a time-dependent flow, but a general indication of the transient mixing process is shown in Fig. 1. The figure shows perspective views of an isosurface of instantaneous c_u, the scalar emitted at the surface. This scalar diffuses upward, filling the boundary layer and reacting with the other component. The distribution is shown for a concentration level of 0.05 at $t = 6000$ s for two reaction rates. For the slow reaction rate, $R = 0.1$, the scalar has largely filled the boundary layer at a level of 0.05, and the only visible features are the downdraft regions where it is removed by the reaction with the entraining species c_d. For the faster reaction, $R = 10$, the scalar is generally destroyed before it can penetrate very far into the mixed layer. The structure of the convective updrafts is clearly evident as they lift the high concentrations out of the surface layer. In the strongest updrafts, the isosurface is lifted up to the inversion, but in the weaker circulations the scalar is reacted away before it can penetrate very far.

The effect of the reaction rate is shown in Fig. 2, where the average statistics of the concentration fields over the time interval from $t = 6000$ to 9000 s are shown. It is obvious that c_u is destroyed more effectively by the faster reaction and that c_d is also reduced in the lower part of the boundary layer where the reaction is primarily conducted. The effects of reaction rate are also evident in the flux profiles, which show that the upward flux of c_u is reduced as the reaction removes the species above the surface layer, while the downward flux of c_d is increased due to the diffusion of the existing boundary layer c_d into the deficit region induced by the reaction near the surface. For the slowest reaction rate, the c_u-flux profile is almost linear, indicating a uniform distribution across the bulk of the mixed layer. Figure 2 also shows the concentration fluctuation variance profiles from the resolved LES results. No subgrid fluctuation estimates have been attempted. The variance in c_u shows limited vertical penetration for fast reaction rates, behavior very similar to the mean value. The variance in c_d shows increasing fluctuation levels in the lower boundary layer as the faster reaction rate produces larger deviations from the initially constant concentration value and a relatively fixed peak at the inversion caused by wavelike disturbances of the gradient at that level.

One of our major interests in conducting these studies is the effect of the turbulent mixing process on the chemical reaction, for which the segregation coefficient s, defined in section 1, provides a direct measure. Profiles of s for the three reaction rates are shown in Fig. 3 for the same averaging period as the statistics in Fig. 2. The reaction rate is seen to induce a strong effect on s, with s tending rapidly toward -1 as the reaction rate increases. This, as expected, demonstrates the controlling effect of the turbulent mixing rate on the reaction. As the reaction becomes faster the species

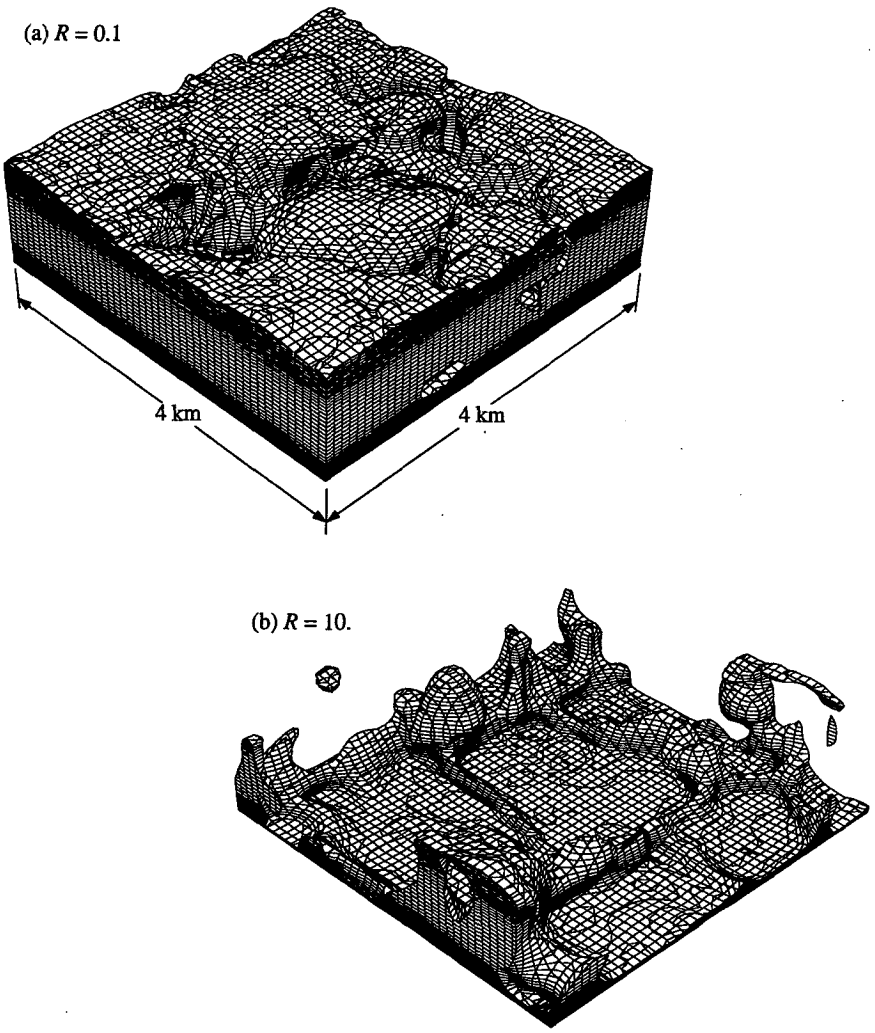

FIG. 1. Instantaneous isosurface of the upward diffusing reactant c_u in a convective boundary layer for (a) $R = 0.1$; (b) $R = 10$. Isosurface value is 0.05. Inversion height is 1 km and $t = 6000$ s.

become increasingly segregated and the overall reaction proceeds much more slowly, by nearly an order of magnitude for $R = 10.0$, than an estimate based solely on the mean concentrations.

The segregation coefficient is also a sensitive test of resolution, especially for fast reactions. The high-resolution calculation with $R = 10$ was made on a grid having nearly twice the resolution of the standard case. As shown in Fig. 3, the segregation coefficient is nearly the same as in the standard case over most of the mixed layer, although near the surface the high-resolution calculation shows greater segregation. This results from better resolution of the small-scale thermal updrafts, which carry unmixed c_u to a greater height than in the standard case. Nonetheless, the small difference in s with resolution gives confidence that the standard case is adequately resolved and that the neglect of subgrid segregation is reasonable throughout most of the mixed layer, though subgrid estimates of s may be important near the surface.

The actual chemical conversion rate profiles are shown in Fig. 4, again illustrating the strong localization of the reaction in the lower boundary layer at fast reaction rates. It is clear that although the reaction rate increases by a factor of 10 between $R = 1$ and 10, the conversion rate is much less sensitive. This can be interpreted as diffusion-limited reaction, where increasing the rate constant cannot increase the overall conversion rate. It also suggests that R is a good definition of the Damköhler number since $R = 1$ appears to correspond roughly to the point where the turbulent diffusion begins to dominate. This is also supported by the similar c_d profiles for $R = 1$ and 10 in Fig. 2.

The complete description of the fluctuating relation between c_u and c_d is provided by the joint probability density function (pdf) for the two quantities. Three

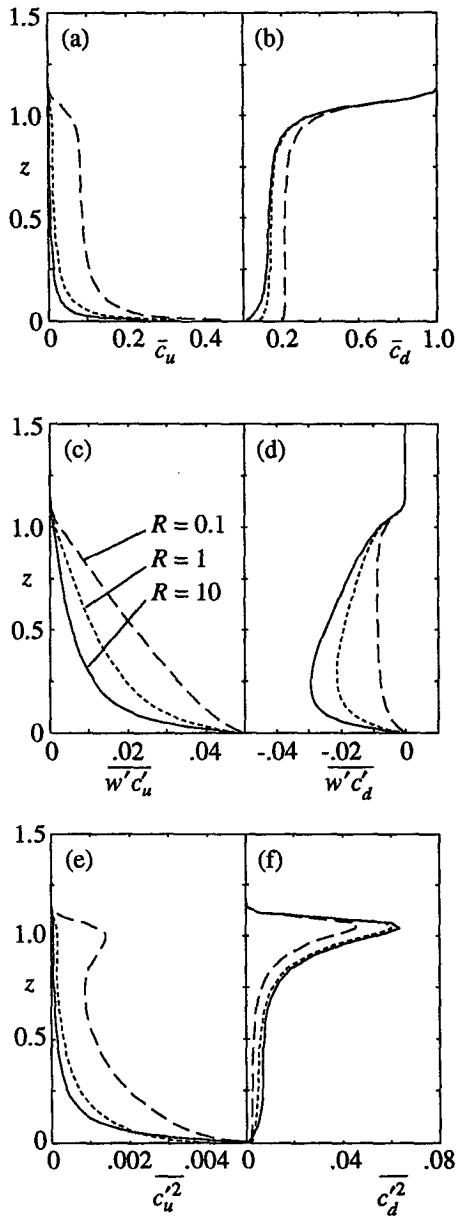

FIG. 2. LES mean reacting scalar profiles for dispersion in a convective boundary layer. Three reaction rates: R = 0.1 (dashed), R = 1.0 (dotted), and R = 10 (solid). Concentration: (a) upward diffusing; (b) downward diffusing, vertical flux; (c) upward diffusing; (d) downward diffusing, scalar variance; (e) upward diffusing; (f) downward diffusing. The averaging period was t = 6000–9000 s; height is in kilometers.

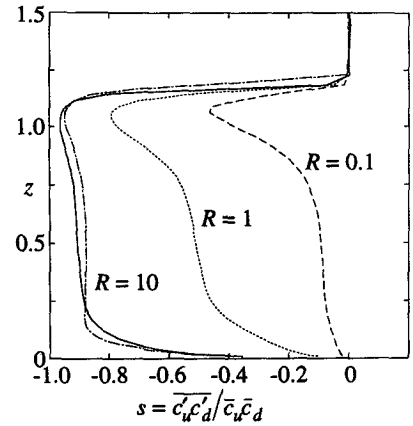

FIG. 3. LES mean segregation coefficient profiles for reacting scalar dispersion in a convective boundary layer. Three reaction rates: R = 0.1 (dashed), R = 1.0 (dotted), R = 10 (solid); high-resolution R = 10 (dash–dot). The averaging period was t = 6000–9000 s.

examples of the joint pdf at z = 100 m, corresponding to the three reaction rates, are shown in Fig. 5. For the slow reaction, the pdf is centered around (0.1, 0.2) in the (c_u, c_d) space with tails extending from 0 to 0.4 in c_u but much more limited in the range of c_d. For the faster reactions, the pdf's are much more confined to the axes where one of the constituents is zero. The only nonzero contributions to the product, $c_u c_d$, come from small values of both species. The segregation of the two reactants is obvious in the pdf where mixing is indicated by nonzero values of both species. The segregation coefficient is a simple measure of this effect. The objective of improved modeling must be to quantify this segregation as a function of the turbulence and the chemistry.

4. One-point closure modeling

Second-order turbulence closure provides a natural framework for describing the segregation effect, since the one-point two-species fluctuation correlation is one of the moments for which a transport equation is included for closure at second-order. The presence of chemical reaction introduces new terms into the species conservation equations, and the nonlinearity of the reaction terms generates a moment hierarchy that re-

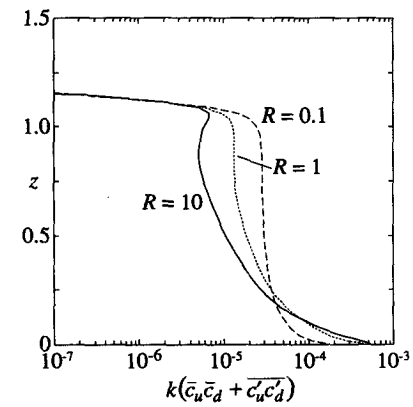

FIG. 4. LES mean total reaction rate profiles for reacting scalar dispersion in a convective boundary layer. Three reaction rates: R = 0.1 (dashed), R = 1.0 (dotted), R = 10 (solid). The averaging period was t = 6000–9000 s.

quires additional closure assumptions in analogy with the nonlinear advective terms. The full closure equations for the second-moment scalar species correlations are written as follows:

$$\frac{D}{Dt}\overline{u_i' c_u'} = -\overline{u_i' u_j'}\frac{\partial \bar{c}_u}{\partial x_j} - \overline{u_j' c_u'}\frac{\partial \bar{u}_i}{\partial x_j} + \frac{g_i}{\theta_0}\overline{c_u'\theta'} + \nu_c \frac{\partial}{\partial x_j}\left(q\Lambda \frac{\partial \overline{u_i' c_u'}}{\partial x_j}\right) - A\frac{q}{\Lambda}\overline{u_i' c_u'} - k(\overline{u_i' c_u' c_d} + \overline{u_i' c_d' \bar{c}_u} + \overline{u_i' c_u' c_d'})$$

$$\frac{D}{Dt}\overline{c_u'\theta'} = -\overline{u_j'\theta'}\frac{\partial \bar{c}_u}{\partial x_j} - \overline{u_j' c_u'}\frac{\partial \bar{\theta}}{\partial x_j} + \nu_c \frac{\partial}{\partial x_j}\left(q\Lambda \frac{\partial \overline{c_u'\theta'}}{\partial x_j}\right) - 2bs_m\frac{q}{\Lambda}\overline{c_u'\theta'} - k(\overline{c_u'\theta'}\bar{c}_d + \overline{c_d'\theta'}\bar{c}_u + \overline{c_u' c_d'\theta'})$$

$$\frac{D}{Dt}\overline{c_u' c_d'} = -\overline{u_j' c_d'}\frac{\partial \bar{c}_u}{\partial x_j} - \overline{u_j' c_u'}\frac{\partial \bar{c}_d}{\partial x_j} + \nu_c \frac{\partial}{\partial x_j}\left(q\Lambda \frac{\partial \overline{c_u' c_d'}}{\partial x_j}\right) - 2bs_m\frac{q}{\Lambda}\overline{c_u' c_d'} - k(\bar{c}_u\overline{c_u' c_d'} + \bar{c}_d\overline{c_u'^2} + \overline{c_u'^2 c_d'}) - k(\bar{c}_d\overline{c_u' c_d'} + \bar{c}_u\overline{c_d'^2} + \overline{c_u' c_d'^2})$$

$$\frac{D}{Dt}\overline{c_u'^2} = -2\overline{u_j' c_u'}\frac{\partial \bar{c}_u}{\partial x_j} + \nu_c \frac{\partial}{\partial x_j}\left(q\Lambda \frac{\partial \overline{c_u'^2}}{\partial x_j}\right) - 2bs_m\frac{q}{\Lambda}\overline{c_u'^2} - 2k(\bar{c}_u\overline{c_u' c_d'} + \bar{c}_d\overline{c_u'^2} + \overline{c_u'^2 c_d'}),$$

with similar equations for $\overline{u_i' c_d'}$, $\overline{c_d'\theta'}$, and $\overline{c_d'^2}$. Standard Reynolds average notation is used, with an overbar denoting the ensemble mean and a prime denoting a fluctuation from the mean. Here, Λ represents the turbulence length scale and $q^2/2$ is the total turbulence energy. The closure model of Lewellen (1977) has been used to represent the standard model terms, with the empirical closure constants $A = 0.75$, $b = 0.125$, $\nu_c = 0.3$, and $s_m = 1.8$. The reactive terms are written in their original form and still require a model for the triple fluctuation correlations $\overline{c_u'^2 c_d'}$ and $\overline{c_u' c_d'^2}$ to be specified.

The conservation equation for the species correlation $\overline{c_u' c_d'}$ includes the chemistry term, $T_u + T_d$ as a source, where

$$T_u = -k(\bar{c}_u\overline{c_u' c_d'} + \bar{c}_d\overline{c_u'^2} + \overline{c_u'^2 c_d'})$$

$$T_d = -k(\bar{c}_d\overline{c_u' c_d'} + \bar{c}_u\overline{c_d'^2} + \overline{c_u' c_d'^2}).$$

The c_u-variance equation contains the term $2T_u$, while the c_d-variance equation includes $2T_d$. In order to close the model equations, we must parameterize the triple fluctuation correlation in terms of the first and second moments. It should be noted that the triple correlations cannot be specified exactly from just the first and second moments alone (Hilst et al. 1973). Prescription of the form for the joint pdf would provide a direct estimate of the triple fluctuation correlation, but we have been unable to determine a simple analytic description of the LES results illustrated in Fig. 5. We therefore suggest a more pragmatic approach and test some very simple empirical models. The LES results provide a set of test data for comparison, although the final test of the closure model should be the prediction of the mean profiles, which involves interaction with the other model processes.

The simplest model for the triple terms would be to ignore them; that is, assume the triple fluctuation correlation is zero. While the triple is definitely not zero, it is conceivably negligible in comparison with the other terms appearing in T_u or similar expressions under some conditions. We can compare the model for the full triple correlation $\overline{c_u^2 c_d}$ with that obtained from the LES statistics for the range of reaction rates. The full average, rather than just the fluctuating part, is the term driving the total reaction. The reaction term in the mean species equation is $-k\bar{c}_u\bar{c}_d$, while in the $\overline{c_u c_d}$ equation it is $-k(\overline{c_u^2 c_d} + \overline{c_u c_d^2})$. The ratio of the model for the triple, that is, ignoring the triple fluctuation correlation, to the LES result is shown in Fig. 6 as a function of segregation coefficient. The singularity as s approaches -1 is obvious in the figure. As $s \to -1$, c_u and c_d are never simultaneously nonzero and the full triple must tend to zero. Ignoring the triple fluctuation implies that the model triple is nonzero. We therefore expect that ignoring the triple fluctuation will cause difficulties in modeling fast reactions where s is close to -1.

An alternative approach is to choose a model to maintain consistency in the limit of an infinite reaction. This requires that

$$\overline{c_u'^2 c_d'} = -(\bar{c}_u\overline{c_u' c_d'} + \bar{c}_d\overline{c_u'^2})$$

when $s = -1$. Hilst et al. (1973) formulated a model that satisfies this requirement but fails to maintain a positive full triple when s is close to -1. A simple model satisfying both requirements is given by

$$\overline{c_u'^2 c_d'} = s(\overline{c_u'^2} + s\bar{c}_u^2)\bar{c}_d \quad \text{(model A)}.$$

We also consider an alternative model, slightly simpler than model A,

$$\overline{c_u'^2 c_d'} = -(\overline{c_u'^2} + s\bar{c}_u^2)\bar{c}_d, \quad \text{(model B)},$$

which also satisfies the realizability condition at $s = -1$. In fact, model B implies that the reaction terms T_u and T_d vanish for all values of s, and is of interest in the limit of very fast reactions. This limit will be discussed in more detail below. In the closure modeling

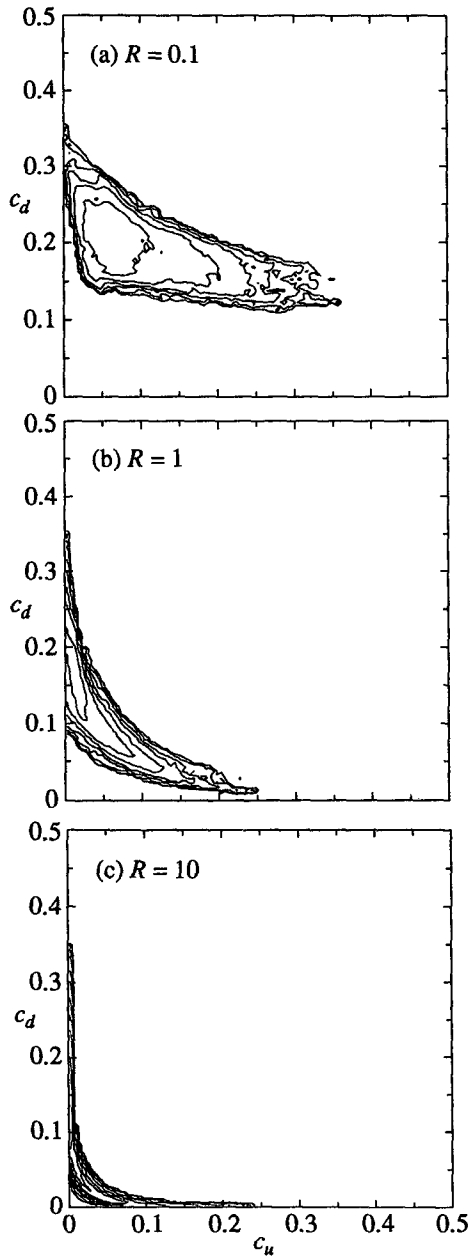

FIG. 5. LES joint pdf's for reacting scalar dispersion in a convective boundary layer at $z = 100$ m and $t = 6000$ s. Three reaction rates: (a) $R = 0.1$, (b) $R = 1.0$, (c) $R = 10$. Logarithmic contour levels of 0.1, 0.3, 1, 3, 10, 30, 100, and 300.

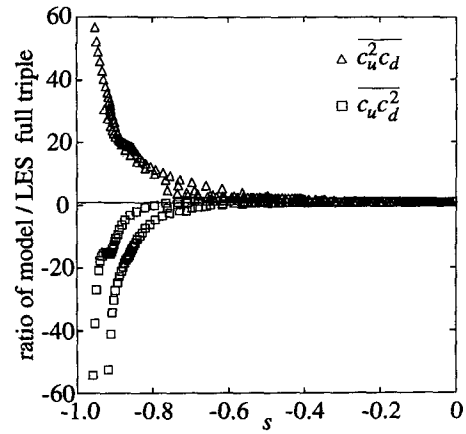

FIG. 6. Ratio of the full triple computed using model C to the LES result: triangle—$\overline{c_u^2 c_d}$; square—$\overline{c_u c_d^2}$.

below, we shall also designate neglecting the fluctuating triple as model C (Fig. 6). Thus,

$$\overline{c_u'^2 c_d'} = 0 \quad \text{(model C)}.$$

We emphasize again that model C does not satisfy the realizability condition when $s = -1$.

The ratio of the full triples obtained using the above models A and B to the LES result are shown in Fig. 7, demonstrating the nonsingular behavior in the limit of fast reaction. The ratio is not accurately unity in the limit for either model, but both models are clearly an improvement over ignoring the fluctuations (model C). Model A is slightly superior over the range of the LES data, maintaining a ratio closer to unity than model B. Both models also maintain positive triples. The performance of the models must be ultimately judged from the results of a full closure model prediction of the reacting mixed-layer evolution.

The LES flow situation has been simulated using the closure model of Lewellen (1977) with additional chemistry terms as appropriate. The triples in the species correlation equations were modeled as described above and new chemistry terms in the velocity and temperature correlation equations were modeled using a similar philosophy. Thus, the reactive terms in the $\overline{w'c_u'}$ equation are

$$-k(\overline{w'c_u'}\bar{c}_d + \overline{w'c_d'}\bar{c}_u + \overline{w'c_u'c_d'}),$$

and this whole term must vanish when $s = -1$. We therefore model

$$\overline{w'c_u'c_d'} = s(\overline{w'c_u'}\bar{c}_d + \overline{w'c_d'}\bar{c}_u)$$

for model A, while model B replaces the leading s with -1. Model C neglects the fluctuating triple entirely. Again, model B implies that the reactive term is identically zero. Similar terms appear in the temperature–species correlation equation.

Results for the mean species profiles, vertical flux profiles, and segregation coefficient profiles are shown

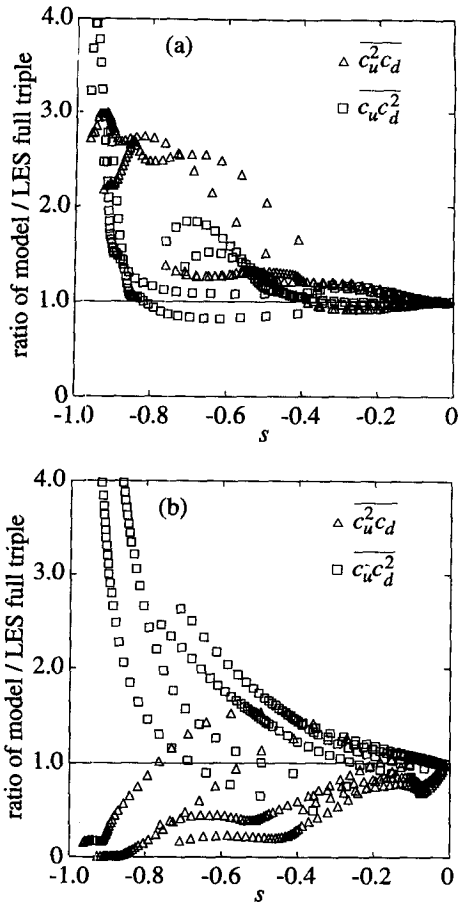

FIG. 7. Ratio of the full triple computed using (a) model A and (b) model B to the LES result: triangle—$\overline{c_u^2 c_d}$; square—$\overline{c_u c_d^2}$.

in Fig. 8 for model A at $t = 7500$ s, and can be compared with the LES prediction in Fig. 2. There are significant differences between the two results, most clearly evident in the vertical penetration of c_u. The LES calculation shows a shallower region and a more complete reaction between the two species as indicated by the smaller value of s near the surface. The one-dimensional ensemble average model maintains a higher segregation near the surface and the reaction therefore proceeds more slowly as the scalar diffuses upward from the surface allowing c_u to penetrate farther into the upper boundary layer. This can be traced, in part, to the greater entrainment of c_d in the LES calculation decreasing its variance and hence the segregation of the species. This makes more c_d available to react with c_u. The agreement in segregation coefficient in the middle region of the boundary layer, where the turbulent fluctuations are better resolved by the LES, is very encouraging in light of the simple modeling used for the reactive triple terms. Figure 9 shows the LES results compared to the model results at an earlier time, where the total scalar masses are more nearly equal, partially eliminating the entrainment effect, and demonstrates much better agreement in the profile shapes.

Differences between the three models for the triple fluctuation term are presented in Fig. 10 for the $R = 10$ case. The most obvious differences are in the flux terms, where model B shows a deeper penetration and model C a shallower penetration in comparison with model A. It is somewhat surprising, in view of the importance of the reactive terms, that these three different models give such similar results.

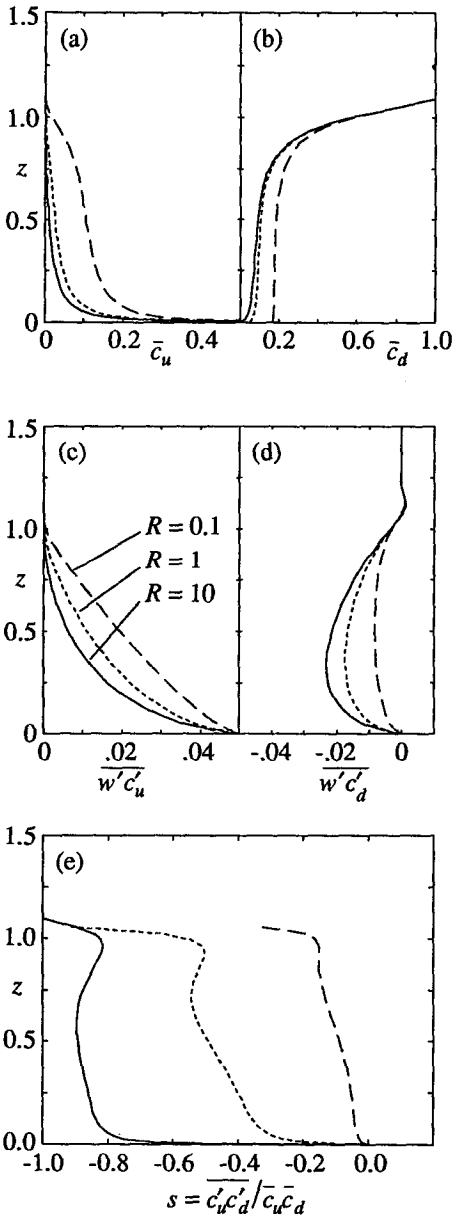

FIG. 8. One-dimensional model reacting scalar profiles for dispersion in a convective boundary layer. Model A results at $t = 7500$ s for three reaction rates: $R = 0.1$ (dashed), $R = 1.0$ (dotted), $R = 10$ (solid). Concentration: (a) upward diffusing; (b) downward diffusing, vertical flux; (c) upward diffusing; (d) downward diffusing; (e) segregation coefficient.

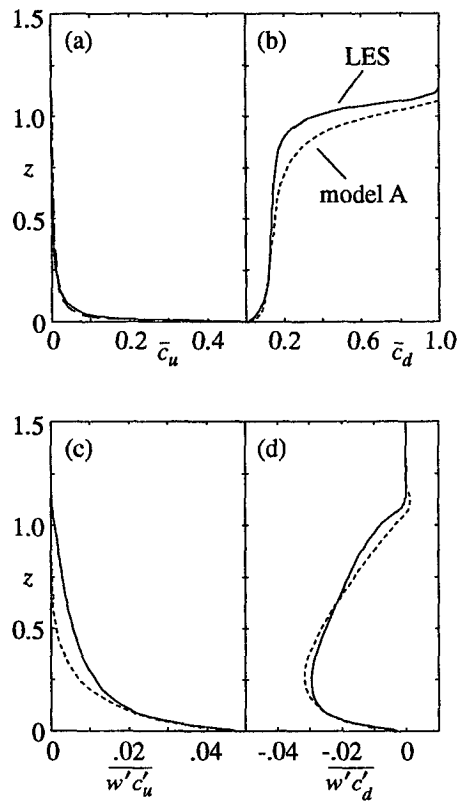

FIG. 9. Reacting scalar profiles for dispersion in a convective boundary layer for $R = 10$. LES mean profiles for $t = 6000$–9000 s (solid); model A profiles at $t = 6000$ s (dotted). Concentration: (a) upward diffusing; (b) downward diffusing, vertical flux; (c) upward diffusing; (d) downward diffusing.

The overall limit on the reaction imposed by the diffusive terms is evidently playing a controlling role and enforcing a similar result for the segregation coefficient. Also shown in the figure are the results of using only the mean reaction term $k\bar{c}_u\bar{c}_d$ in the mean species equations, that is, assuming $s = 0$. The shallower c_u penetration and smaller mixed-layer value of c_d are consistent with a faster overall reaction rate and support the importance of correctly predicting the segregation.

A more critical distinction between the various models for the fluctuation triple term is found in the limit of an infinite reaction rate, $k \to \infty$. The detailed behavior in the limit $s \to -1$ is the determining factor for the effective reaction rate, as the following analysis reveals. A simple expression for the effective reaction rate can be obtained from the equation for $\overline{c_u c_d}$, which must vanish as $k \to \infty$. If we ignore the gradient production terms and the turbulent diffusion terms, a balance between the reactive terms and the dissipation rate is obtained as

$$-k\overline{c_u c_d}(\bar{c}_u + \bar{c}_d) + T_1 + T_2 - 2bs_m \frac{q}{\Lambda}\overline{c'_u c'_d} = 0.$$

We solve for the effective reaction rate $k\overline{c_u c_d}$ and invoke the limit $s = -1$ to replace $\overline{c'_u c'_d}$ by $-\bar{c}_u\bar{c}_d$. Model B immediately yields

$$k\overline{c_u c_d} = 2bs_m \frac{q}{\Lambda}\frac{\bar{c}_u\bar{c}_d}{(\bar{c}_u + \bar{c}_d)},$$

which is very similar to the model of Varma et al. (1977), where the rate is proportional to the smaller concentration as one of the species disappears. The timescale for the reaction is the turbulent timescale, as expected in a diffusion limited system. The result for model A is slightly more complicated but is readily obtained as

$$k\overline{c_u c_d} = 2bs_m \frac{q}{\Lambda}\frac{\bar{c}_u\bar{c}_d}{[(\overline{c'^2_u}/\bar{c}_u) + (\overline{c'^2_d}/\bar{c}_d)]}.$$

In this case, the reaction is determined by the fluctuation intensity and is less easily generalized. For model C, no such balance is possible. Further study of the fast reaction limit is necessary to determine the most appropriate model formulation.

5. Conclusions

Large-eddy simulations of chemically reactive mixing of two species in the convectively driven mixed layer have produced detailed statistics of the fluctuating concentration fields. The situation under consideration is the emission of one reactant c_u into a uniformly mixed layer containing a second reactant c_d. This situation has been previously studied using LES by Schumann (1989). The results have been analyzed from the perspective of the effects of turbulent mixing on the effective reaction between the species. The segregation between the species was shown to be significant for fast reactions, and therefore correct model predictions of the evolution of the constituent concentrations require an estimate of the segregation coefficient. Profiles of fluctuation correlations and the joint pdf of the two reacting species have been examined. The effect of fast reaction is to limit the penetration of c_u into the mixed layer, and also to increase the segregation between the two species.

Some simple modeling concepts for one-point closure schemes have been examined and compared with the LES predictions. An important requirement for the fast reaction situation appears to be the realizability condition that

$$\overline{c_u^2 c_d} \to 0 \text{ as } \overline{c_u c_d} \to 0,$$

which occurs as the reaction rate constant becomes large. The application of the simple closure model in a full one-dimensional boundary layer calculation produced reasonably accurate predictions of the mean species evolution. The results are a promising indication that second-order closure schemes can be extended to provide a practical calculation of turbulent mixing effects on fast chemical reactions.

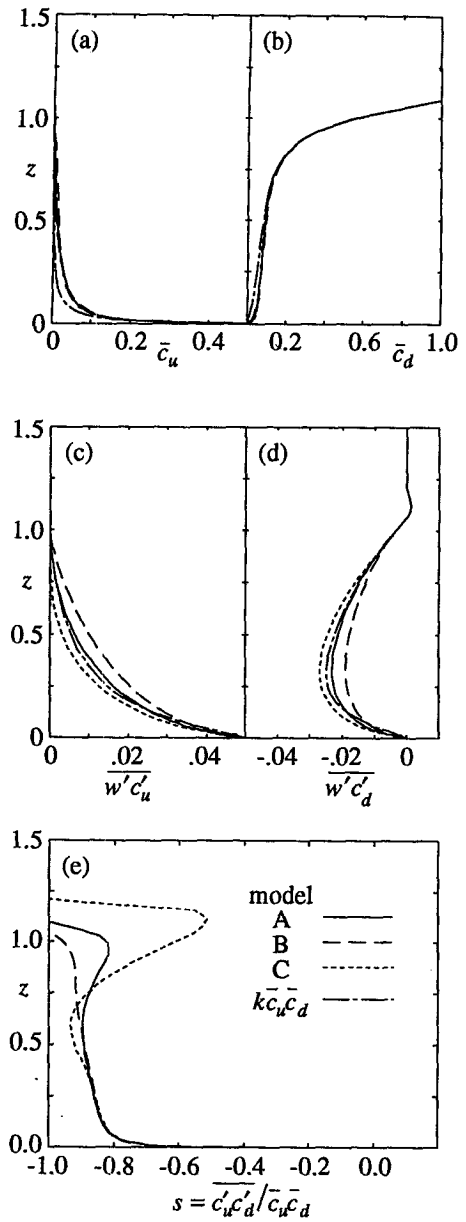

FIG. 10. One-dimensional model reacting scalar profiles for dispersion in a convective boundary layer for $R = 10$ and $t = 7500$ s. Results from three models: model A (solid), model B (dashed), model C (dotted), and mean reaction term only (dash–dot). Concentration: (a) upward diffusing; (b) downward diffusing, vertical flux; (c) upward diffusing; (d) downward diffusing; (e) segregation coefficient.

The form of the triple correlation model is important in determining the behavior for fast reactions. For the simple models considered, the limiting reaction rate for an infinite rate constant has been derived. One model yields the simple result of Varma et al. (1977), which depends only on the mean concentrations, while the other model depends on the concentration fluctuation intensity as well. Further investigation into diffusion-limited reactions is required to distinguish the relative merits of the two models.

Acknowledgments. This work was supported by the Office of Naval Research under Contract N00014-92-C-0058.

REFERENCES

Arellano, J. V.-G. d., A. M. Talmon, and P. J. H. Builtjes, 1990: A chemically reactive plume model for the NO–NO_2–O_3 system. *Atmos. Environ.*, **24A,** 2237–2246.

Bange, P., L. H. J. M. Jansen, F. T. M. Nieuwstadt, H. Visser, and J. J. Erbrink, 1991: Improvement of the modelling of daytime nitrogen oxide oxidation in plumes by using instantaneous plume dispersion parameters. *Atmos. Environ.*, **25A,** 2321–2328.

Carpenter, R. L., K. K. Droegemeier, P. R. Woodward, and C. E. Hane, 1990: Application of the piecewise parabolic method (PPM) to meteorological modeling. *Mon. Wea. Rev.*, **118,** 586–612.

Carter, W. P. L., and F. W. Lurmann, 1991: Evaluation of a detailed gas-phase atmospheric reaction mechanism using environmental chamber data. *Atmos. Environ.*, **25A,** 2771–2806.

Collela, P., and P. R. Woodward, 1984: The piecewise parabolic method (PPM) for gas-dynamical simulations. *J. Comput. Phys.*, **54,** 174–201.

Donaldson, C. du P., and G. R. Hilst, 1972a: Chemical reaction in inhomogeneous mixtures: The effect of the scale of turbulent mixing. *Proc. 1972 Heat Transfer and Fluid Mechanics Institute,* R. B. Landis and G. J. Hordemann, Eds., Stanford University Press, 253–261.

——, and ——, 1972b: Effect of inhomogeneous mixing on atmospheric photochemical reactions. *Environ. Sci. Technol.*, **6,** 812–816.

Henn, D. S., and R. I. Sykes, 1992: Large-eddy simulation of dispersion in the convective boundary layer. *Atmos. Environ.*, **26A,** 3145–3159.

Hilst, G. R., C. d. P. Donaldson, M. E. Teske, R. M. Contiliano, and J. Freiberg, 1973: The development and preliminary application of an invariant coupled diffusion and chemistry model. NASA CR-2295, Langley Research Center, National Aeronautics and Space Administration, Washington, D.C., 83 pp. [NTIS N7330106.]

Lewellen, W. S., 1977: Use of invariant modeling. *Handbook of Turbulence,* W. Frost and T. H. Moulden, Eds., Plenum, 237–279.

Mellor, G. L., and T. Yamada, 1974: A hierarchy of turbulence closure models for planetary boundary layers. *J. Atmos. Sci.*, **31,** 1791–1806.

Schumann, U., 1989: Large-eddy simulation of turbulent diffusion with chemical reactions in the convective boundary layer. *Atmos. Environ.*, **23,** 1713–1727.

Seigneur, C., P. Saxena, and V. A. Mirabella, 1985: Diffusion and reaction of pollutants in stratus clouds: Application to nocturnal acid formation in plumes. *Environ. Sci. Technol.*, **19,** 821–828.

Seinfeld, J. H., 1986: *Atmospheric Chemistry and Physics of Air Pollution.* Wiley, 738 pp.

Sykes, R. I., and D. S. Henn, 1989: Large-eddy simulation of turbulent sheared convection. *J. Atmos. Sci.*, **46,** 1106–1118.

——, and ——, 1992: Large-eddy simulation of concentration fluctuations in a dispersing plume. *Atmos. Environ.*, **26A,** 3127–3144.

——, ——, S. F. Parker, and W. S. Lewellen, 1992: Large-eddy simulation of a turbulent reacting plume. *Atmos. Environ.*, **26A,** 2565–2574.

Varma, A. K., E. S. Fishburne, and R. A. Beddini, 1977: A second-order-closure analysis of turbulent diffusion flames. NASA/LRC, NASA CR-145226, 85 pp. [NTIS N7816118.]

Willis, G. E., and J. W. Deardorff, 1974, A laboratory model of the unstable planetary boundary layer. *J. Atmos. Sci.*, **31,** 1297–1307.